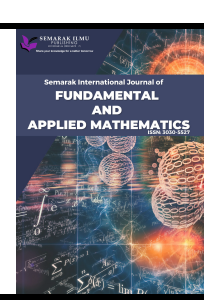


Semarak International Journal of Fundamental and Applied Mathematics

Journal homepage: https://semarakilmu.my/index.php/sijfam ISSN: 3030-5527



Interpolation Based Technique in Evaluating Polarization Tensor of Second Rank in 3D Domains

Nurfarrisha Asnida Khairul Akmar¹, Nurul Alesyah Sairin¹, Haziq Dani Mohammad Azmi¹, Taufiq Khairi Ahmad Khairuddin¹, Suzarina Ahmed Sukri^{1,*}, Yeak Su Hoe¹

1 Department of Mathematical Sciences, Faculty of Science, Universiti Teknologi Malaysia, 81310 Skudai, Johor, Malaysia

ARTICLE INFO

ABSTRACT

Article history:

Received 11 August 2025 Received in revised form 25 August 2025 Accepted 31 August 2025 Available online 7 October 2025

Keywords:

Numerical integration; polarization tensor; linear element

This paper presents a numerical framework for evaluating the polarization tensor (PT) of second rank for three-dimensional object inclusion, where PT is a fundamental tool to modelling the object inclusion response toward an external field. Our proposed method is to approximated the boundary integral formulation of PT using interpolation points, which can reduce the numerical quadrature error and lowering the computational cost. This paper also includes the theoretical validation of the method's accuracy through a proposition from the previous research, ensuring the mathematical formulation is reliable. This integration of computational efficiency together with the validation provides a robust and reliable framework of PT evaluation.

1. Introduction

Interpolation method are a simple yet effective approach to determining second-rank polarization tensors in three-dimensional vectors, and offer the advantage of controlling numerical errors which receives high applicability in engineering and applied sciences. The polarization tensor is a critically important mathematical tool for object where PT able to capture the geometrical and physical characteristics of a material or object; it allows for the characterization of the associations that an applied field has on a material to the resulting disturbance in the applied field, and provides information about the shape, orientation, and internal properties of internal inclusions or other heterogeneities within a spatial domain. Polarization tensors represent a vital albeit complex link in characterizing the requirement of micro-structure to macro-physical behaviour of materials or media, and are necessary for applied fields such as material science, electromagnetics, and applied physics [1,3].

Recent work has opened new insight for the understanding and use of polarization tensors beyond classical problems. For example, polarization tensor ideas have been applied to characterize spin alignment in quantum systems [18], and to investigate nonlinear coupling phenomena in

E-mail address: suzarina@utm.my

_

https://doi.org/10.37934/sijfam.8.1.3846

^{*} Corresponding author.

multiferroic and magnetoelectric materials [12]. Additionally, polarization tensors are utilized in a variety of contexts ranging from electromagnetic theory to astrophysics [13], indicating their potential to evolve across many different contexts. These developments provide motivation to continue developing interpolation-based numerical methods as a way to improve our knowledge about the evaluation of polarization tensors with particular attention to ensuring accurate and efficient computations in various contexts for both researchers and practitioners in physics and engineering.

1.1Interpolation based and Numerical Methods for Polarization Tensor Evaluation

Several interpolation and numerical methods have been developed to evaluate polarization tensors, but few are capable of balancing accuracy, efficiency, and geometric complexity. Gaussian quadrature applied in conjunction with linear element interpolation is a common approach, which uses the contents of a weighted Gaussian quadrature to provide an estimate of the integral of the polarization tensor over a mesh with Gaussian quadrature points. It has been improved, through error analysis and perturbation theory via Taylor expansion, by allowing real-time error estimates to the user as well as the expected error, while performing the numerical computations [10]. This improvement is essential for the highly oscillatory, and rapidly changing fields involved in tensor evaluations. Examples of other capable methodologies include spatial neural networks and meshless interpolation, such as radial basis functions (RBF). Tensor Weave 1.0 is an example of a neural network interpolation method that used physical laws to provide a representative tensor field based on a sparse or irregular distribution of data [9]. RBF methods helped to model the polarization tensor as RBFs can be used on arbitrary geometries without the need for meshes, which can enhance numerical stability and convergence properties [5]. Additionally, there has been the application of polynomial interpolation methods to first-order polarization tensors, particularly least-squares fitting, which evaluate the tensor components, by fitting multivariate polynomials to the data for smoothness and improve convergence for a noisy or discrete input [16]. Research has also shown that using polynomial interpolation combined with Gaussian quadrature enhances accuracy and numerical stability for tensor evaluations for standard geometries such as spheres and ellipsoids [15]. Looking ahead, employing these methods to extend to second-rank polarization tensors in 3D domains appears to have significant potential albeit with greater complexity and precision to consider. Overall, with these interpolation and numerical methods, there is a strong basis for rapid and robust evaluation of polarization tensors in the modern context of computational science and engineering.

1.2 Application of Polarization Tensor

Polarization Tensors (PT) are remarkable tools that can be used to represent the shape, orientation and material properties of inclusions in a host medium. They can be utilized in many applications in industry as well as science. Polarization Tensors (PT) are key tools in electromagnetics and materials science, and are routinely used to simulate and control electromagnetic wave behavior. As tensors they are apt for sophisticated metasurface designs, focusing on dual-band transmissive polarization converters and toroidal dipole—assisted electromagnetically induced transparency (EIT)-enabled polarization control, that achieved stability and efficiency for electromagnetic applications such as communications, received optical filtering, and satellite radar [20]. In the spatial spectral domain methods, Hermite interpolation methods were developed for the pavement of PT calculations on multilayered media, resulting in a much higher order of continuity and differentiability compared to typical basis functions, which improved accuracy and numerical

stability verified with finite element and rigorous coupled wave analysis [6]. In fact, when PTs are applied in electromagnetics, they can be used to describe how inclusions deform fields in a host medium, by describing the shapes, orientations and material properties of the inclusions. They are already a useful tool in electrical impedance tomography (EIT) and electromagnetic imaging in finding objects such as tumors or hidden metal, and are also a cost-effective method and an obviously an easier computational approach than full reconstructions [1]. They also underly eddy current and metal detection instruments with their basic electromagnetic "fingerprint" information for conductive objects.

In materials science, PTs connect microscopic inclusion properties to macroscopic phenomena such as conductivity, permittivity, and permeability. Spheroidal inclusion analytical and numerical studies have validated polarization response predictions and anisotropy in materials [20]. PT estimates using the discretization of boundary element methods (BEM) obtain a high precision that has become benchmark datasets used for comparison and validation of imaging algorithms used in both medical and geophysical applications. For example, electrifield imaging techniques (EIT) which use PTs, have non-invasive imaging methods for medical diagnostics of lung monitoring, detecting breast tumors, or visualization of brain activity. Additionally, PTs assist geoscience to locate groundwater, minerals and geological faults and are a comparison and validation training dataset for machine learning models developed for inversion pipelines. Seismic exploration uses polarization analysis methods [17] that classify wave types based on covariance matrix eigenanalysis, which indirectly uses the PT structure to perform filtering of noise as well as improve signal-to-noise ratios relative to each wave type, for subsurface imaging. Optical methods such as permittivity tensor imaging (PTI) [19] enable visualization of anisotropic properties of biological tissues in threedimensions. In particular for cervical cancer screening, impressive results reveal that dual-modality imaging combining bright-field and polarization would improve sensitivity and accuracy of detecting lesions by quantifying polarimetric parameters [7]. Similarly, Mueller matrix based PTI [11] helps to separate glioma tissue in brain imaging, improving tumor visualization and aiding surgical navigation. Lastly, PTs have a major role in non-destructive testing and inverse problem modelling. PT formulations are valid for detecting and characterizing defects in conductive media. In summary, PTs are useful and compare well technically for modelling electromagnetic responses of complex systems, with a substantial applied impact made in biomedical imaging, metamaterial design, composite material characterization, geophysics, and non-destructive testing.

2. Mathematical Framework for Polarization Tensor

2.1 Equation of PT

In order to solve the transmission problem of PT, the numerical integration of the linear element of Gaussian quadrature, which involves three nodal points, has been implemented in the form of a boundary integral equation. Let V_x denote the outward normal vector to the boundary ∂B at X, and K_B^* is a singular integral operator. While, K_B^* is the integral that is shown below as the P.V. integral and the Cauchy Principal Value

$$K_B^* \phi(X) = \frac{1}{4\pi} P. V. \int_{\partial B} \frac{\langle X - Y \rangle. \langle V_X \rangle}{|X - Y|^3} \phi(Y) d\sigma(Y), \tag{1}$$

where P.V. denotes the principal value integral, ∂B represent the boundary of the domain B while $\phi_i(Y)$ is the surface potential where it can be represented as

$$\phi_i(Y) = (\lambda I - K_B^*)^{-1} (V_X \cdot \nabla X^i)(Y), \tag{2}$$

for which λ is a spectral parameter which is defined in terms of conductivity of the object,

$$\lambda = \frac{k+1}{2k-2},$$

while the conductivity of the object must be in the range of $0 \le k \ne 1 \le +\infty$. Conductivity, k is said to be in the same conductivity of its surrounding if it is equal to 1. By evaluating Eq. (1) and Eq. (2), the integral of first order PT, M_{ij} is evaluated using the following integral.

$$M_{ij}(k,B) = \int_{\partial B} Y^{j} \phi_{i}(Y) d\sigma(Y), Y \in \partial B.$$
 (3)

From Eq. (3), as the linear element being implemented, the equation will be represented in term of summation where it will be further explained in section 2.3. For the next section, the analytical solution which has been derived by Ammari et al., [3].

2.2 Analytical Solution of PT

Although the derivation of the singular integrand of PT can be quite challenging, but, previous researchers has provided the analytical solution for two different geometries, which are sphere and ellipsoid. This analytical solution can become a benchmark for the applicability of the proposed numerical method, which is linear element numerical integration. The derivation of the analytical solution can be read in Ammari and Kang (2007). The researchers derived and represented the final PT equation as a matrix system with 3×3 dimension as in the following equation

$$M(k,B) = (k-1)|B| \begin{bmatrix} \frac{1}{(1-f_1)+kf_1} & 0 & 0\\ 0 & \frac{1}{(1-f_2)+kf_2} & 0\\ 0 & 0 & \frac{1}{(1-f_3)+kf_3} \end{bmatrix}.$$
 (4)

where |B| is the volume of object B while f_1 , f_2 and f_3 is constant defined by integral as

$$f_{1} = \frac{bc}{a} \int_{1}^{+\infty} \frac{1}{t^{2} \sqrt{t^{2} - 1 + \left(\frac{b}{a}\right)^{2}} \sqrt{t^{2} - 1 + \left(\frac{c}{a}\right)^{2}}} dt,$$

$$f_{2} = \frac{bc}{a} \int_{1}^{+\infty} \frac{1}{\left(t^{2} - 1 + \left(\frac{b}{a}\right)^{2}\right)^{\frac{3}{2}}} \sqrt{t^{2} - 1 + \left(\frac{c}{a}\right)^{2}} dt,$$

$$f_{3} = \frac{bc}{a} \int_{1}^{+\infty} \frac{1}{\sqrt{t^{2} - 1 + \left(\frac{b}{a}\right)^{2}} \sqrt{t^{2} - 1 + \left(\frac{c}{a}\right)^{2}}} dt.$$
(5)

Here, a, b and c are semi principle axes of an ellipsoid represented by $x^2/a^2 + y^2/b^2 + z^2/c^2 = 1$ such that $a \ge b \ge c \ge 0$. Matrix system in (20) is used in order to compute the numerical solution of ellipsoid as well as validate the results obtained in this study. By taking semi principle axes become

equal to each other which is a=b=c it will then become the analytical solution for sphere which can be represented as

$$M(k,B) = (k-1)|B| \begin{bmatrix} \frac{3}{2+k} & 0 & 0\\ 0 & \frac{3}{2+k} & 0\\ 0 & 0 & \frac{3}{2+k} \end{bmatrix}.$$
 (6)

Both analytical solutions of the sphere and ellipsoid are used in order to validate the method that has been proposed. These solutions are used as a first benchmark for other complex geometry for which the analytical solution is unknown and probably not exist. For the next section, in order to observe the accuracy of the numerical solution, we presented the formula to compute the error for first order PT.

2.2 Linear Element Integration

Throughout this paper, we intend to implement interpolation technique in order to solve the integral of PT. Then we validate our numerical computation of PT by using proposition that will be stated in the Result and Discussion section. The computation of PT involves the computation of the singular integral in terms of Cauchy Principal integral, K_B^* followed by solving the linear system of $\phi_i(Y)$ and lastly the integral of PT itself. First, the singular integral in Eq. (1) is expressed as the integral containing surface projection, $S_p(\xi,\eta)$ as well as Jacobian, $J(\xi,\eta)$ in terms of local coordinates system.

$$K_B^* \phi(X) = \frac{1}{4\pi} P. V. \int_{\partial B} \frac{\langle X - Y \rangle. \langle V_X \rangle}{|X - Y|^3} \phi(Y) S_p(\xi, \eta) J(\xi, \eta) d\xi d\eta.$$
 (7)

In this case, X and Y is the elements located at the object inclusion

$$\begin{split} \langle X^1 - Y^{1 \dots N} \rangle &= \langle x_1^1 - x_2^{1 \dots N}, y_1^1 - y_2^{1 \dots N}, z_1^1 - z_2^{1 \dots N} \rangle, \\ \langle X^2 - Y^{1 \dots N} \rangle &= \langle x_1^2 - x_2^{1 \dots N}, y_1^2 - y_2^{1 \dots N}, z_1^2 - z_2^{1 \dots N} \rangle, \\ &\vdots \\ \langle X^{1 \dots N} - Y^{1 \dots N} \rangle &= \langle x_1^{1 \dots N} - x_2^{1 \dots N}, y_1^{1 \dots N} - y_2^{1 \dots N}, z_1^{1 \dots N} - z_2^{1 \dots N} \rangle \end{split}$$

while X-Y is the distance between the barycentre of element X (containing x,y and z coordinates) to element Y (containing x,y and z coordinates). Let X_1 be the first element of the object inclusion with Y_2 be the second element of the object inclusion. This inner product will yield to

$$\frac{\langle X - Y \rangle . \langle V_X \rangle}{|X_1 - Y_2|^3} = \begin{bmatrix}
\frac{\langle X^1 - Y^1 \rangle \cdot V_{X_{1..3}}^1}{|X^1 - Y^1|^3} & \dots & \frac{\langle X^1 - Y^N \rangle \cdot V_{X_{1..3}}^1}{|X^1 - Y^N|^3} \\
\vdots & \ddots & \vdots \\
\frac{\langle X^N - Y^1 \rangle \cdot V_{X_{1..3}}^N}{|X^N - Y^1|^3} & \dots & \frac{\langle X^N - Y^N \rangle \cdot V_{X_{1...3}}^N}{|X^N - Y^N|^3}
\end{bmatrix}_{N \times N}$$
(8)

It will then being dot product with the outward normal vector of element X, $V_X = \langle V_{X_1}, V_{X_2}, V_{X_3} \rangle$ for which V_{X_1}, V_{X_2} and V_{X_3} be the x, y and z coordinates for normal vector of element X. From Eq. (7), the surface projection, $S_n(\xi, \eta)$ is expressed as

$$S_p(\xi, \eta) = \frac{\langle x_i, y_i, z_i \rangle}{|\langle x_i, y_i, z_i \rangle|} \tag{9}$$

while

$$J(\xi,\eta) = \begin{bmatrix} x_{\xi} & x_{\eta} \\ y_{\xi} & y_{\eta} \\ z_{\xi} & z_{\eta} \end{bmatrix} = \begin{bmatrix} x_{13} & x_{23} \\ y_{13} & y_{23} \\ z_{13} & z_{23} \end{bmatrix}$$
(10)

By substituting Eq. (8), (9) and (10), Eq. (7) is expressed in terms of summation form

$$K_B^*\phi(X) = \frac{1}{4\pi} P. V. \sum_{k=1}^N \frac{\langle X_i^k - Y_j^k \rangle. \langle V_{X_i} \rangle}{\left| X_i - Y_j \right|^3} \phi(Y_j) S_p(\xi, \eta) J(\xi, \eta), \tag{11}$$

where the size of K_B^* is $N \times N$. From the solution of K_B^* , we substitute it into linear system in (2) and finally we obtained the integral of PT as in Eq. (12).

$$M_{ij}(k,B) = \sum_{k=1}^{N} \sum_{q=1}^{3} W_q Y^k \phi(Y^k) J(\xi,\eta),$$
(11)

The following section presents the result of first order PT where we compute the first order PT for a sphere and instead of validating the solution with the analytical solution as conducted by Sukri *et al.*, [15], we use proposition to show that the proposed method is reliable to be implemented.

3. Results and Discussion

Previous theoretical findings show that the first order polarization tensor (PT) is depends on the scaling factors, f_s which related to the size of the reference object. To approximate the first order PT, two methods are used to calculate PT for sphere geometry with a constant conductivity value for

different geometry sizes. This approach is based on proposition from Hyeonbae Kang (2013), which explains the transformation formula of PT with f_s .

Proposition 3.1 Given that M(k,B) is the first order PT for the referred geometry B. Let f_s be the scaling factors for the size of object B. The first order PT for B after its size is scaled, $M(k,f_s,B)$ satisfies $M(k,f_s,B) = f_s^3 M(k,B)$

Proposition 3.1 states that the first order PT of the original geometry can be used to determine the PT after the geometry has been scaled. This information is important for validating numerical computations when dealing with the objects with no analytical solutions. For standard shapes like spheres or ellipsoid, are more straightforward to verify because analytical solution is provided. However, for other shapes, we need to ensure that the numerical results follow the transformation formula in proposition 3.1. If the computed PT fulfil this transformation, we can assume the solution is accurate, and the method used is reliable for evaluating the first order PT. In general, the PT can be calculated using numerical methods. In this study, we compute the first order PT using an approach based on the integration of linear elements. We begin by presenting the numerical results of the first order PT for a sphere, using a few different size scales. The conductivity is fixed at 0.5 and different radius which is r=0.5 and 1. Theoretical values of first order PT are then calculated for comparison. For each sphere with different value of radius, the norm of the first order PT is shown 3.1 where the matrix norm is calculated using formula ||M(k,B)|| = $\sqrt{M_{11}^2 + M_{12}^2 + \dots + M_{32}^2 + M_{33}^2}$ in which $||M(k, B)|| = ||M(k, B)||_2$.

Table 1 The norm of the first order PT for a sphere with different radius, r when conductivity k=0.5

Radius, r	Centre	M(k,B)
0.5	(0,0,0)	0.4307267218
	(0,1,0)	0.4542677484
	(0,0,1)	0.4272636527
1	(0,0,0)	3.440584793
	(0,1,0)	3.525823421
	(0,0,1)	3.573473194

Table 1 presents the norms of the first order PT for sphere with different radius where it can be observed that, for smaller radius of sphere, the PT norms measured at different centres shows values around 0.43 to 0.45. Differently with spheres with larger radius, which exhibits significantly higher norms ranging approximately from 3.44 to 3.57. These reflect the increasing magnitude of PT norm as the radius of sphere increase, which aligns with the theoretical understanding that the larger inclusion induces a strong polarization effects. Additionally, the slight variations in PT norms at different centres points highlight the directional sensitivity or minor anisotropic behaviour inherent in the measurements or calculations.

Table 2 The comparison for actual and the norm of the first order PT for the sphere with different radius r when conductivity k=0.5

Radius, r	Actual PT, $M(k, f_s B)$	Computed PT $M(k, B)$	Absolute Error $ M(k, f_s B) - M(k, B) $
0.5	0.4300730991	0.4307267218	0.0006536227
	0.4407279276	0.4542677484	0.0135398208
	0.4466841493	0.4272636527	0.0194204966
1	3.445813774	3.440584793	0.005228981
	3.634141987	3.525823421	0.108318566
	3.418109222	3.573473194	0.155363972

4. Conclusions

In conclusion, this paper has introduced an interpolation based framework for evaluating polarization tensor for 3D object inclusion where its reliability is supported by theoretical validation through previous proposition. The results confirm that the method is consistent, aligning with the formulation established by previous researcher. However, while the approach achieves notable computational efficiency, its accuracy is limited. As a future research direction, the incorporation of higher order interpolation is recommended to further enhance the efficiency and accuracy.

Acknowledgement

This research was funded by a grant from Universiti Teknologi Malaysia (UTM) for the financial funding under UTM Encouragement Research (UTMER) grant scheme with reference number PY/2024/00856 and cost centre number Q.J130000.3854.42J43.

References

- 1] Khairuddin, Taufiq Khairi Ahmad, and William RB Lionheart. "Polarization tensor: Between Biology and engineering." *Malaysian Journal of Mathematical Sciences* 10 (2016): 179-191.https://mjms.upm.edu.my/fullpaper/2016-March-10(S)/Taufiq%20Khairi%20Ahmad%20Khairuddin-179-191.pdf
- [2] Amad, Alan AS, Paul D. Ledger, Timo Betcke, and Dirk Praetorius. "Benchmark computations for the polarization tensor characterization of small conducting objects." *Applied Mathematical Modelling* 111 (2022): 94-107. https://doi.org/10.1016/j.apm.2022.06.024
- [3] Ammari, Habib, Hyeonbae Kang, and Mikyoung Lim. "Polarization tensors and their applications." In *Journal of Physics: Conference Series*, vol. 12, no. 1, p. 13. IOP Publishing, 2005. https://doi.org/10.1088/1742-6596/12/1/002
- [4] Bordag, M., G. L. Klimchitskaya, and V. M. Mostepanenko. "Convergence of the polarization tensor in spacetime of three dimensions." *Physical Review D* 109, no. 12 (2024): 125014. https://doi.org/10.1103/PhysRevD.109.125014
- [5] Blarr, Juliane, T. Sabiston, Constantin Krauß, Julian Karl Bauer, W. V. Liebig, K. Inal, and Kay André Weidenmann. "Implementation and comparison of algebraic and machine learning based tensor interpolation methods applied to fiber orientation tensor fields obtained from CT images." *Computational Materials Science* 228 (2023): 112286. https://doi.org/10.1016/j.commatsci.2023.112286
- [6] Dilz, Roeland J., and Martijn C. van Beurden. "A Hermite-interpolation discretization and a uniform path deformation for the spatial spectral domain integral equation method in multilayered media for TE polarization." Progress In Electromagnetics Research B 80 (2018): 37-57. https://doi.org/10.2528/PIERB17112104
- [7] Dong, Yang, Jiachen Wan, Xingjian Wang, Jing-Hao Xue, Jibin Zou, Honghui He, Pengcheng Li, Anli Hou, and Hui Ma. "A polarization-imaging-based machine learning framework for quantitative pathological diagnosis of cervical precancerous lesions." *IEEE Transactions on Medical Imaging* 40, no. 12 (2021): 3728-3738. https://doi.org/10.1109/TMI.2021.3097200
- [8] Fukushima, Kenji, Yoshimasa Hidaka, and Tomoya Uji. "Photon polarization tensor at finite temperature and density in a magnetic field." *Journal of High Energy Physics* 2025, no. 5 (2025): 1-29. https://doi.org/10.48550/arXiv.2411.09994
- [9] Kamath, Akshay V., Samuel T. Thiele, Hernan Ugalde, Bill Morris, Raimon Tolosana-Delgado, Moritz Kirsch, and Richard Gloaguen. "TensorWeave 1.0: Interpolating geophysical tensor fields with spatial neural networks." *EGUsphere* 2025 (2025): 1-26. <a href="https://ht
- [10] Akmar, Nurfarrisha Asnida Khairul, Suzarina Ahmed Sukri, and Hoe Yeak Su. "Interpolation Technique in Solving Second Rank Polarization Tensor with Error Analysis." *Malaysian Journal of Fundamental and Applied Sciences* 21, no. 3 (2025): 2111-2119. https://doi.org/10.11113/mjfas.v21n3.4143
- [11] Liu, Yi-Rong, Chao-Feng Liang, Han-Qiao Zhao, Yun-Mou Ou, and Jian Wu. "A polarization image enhancement method for glioma." *Frontiers in Neuroscience* 17 (2023): 1163701. https://doi.org/10.3389/fnins.2023.1163701
- [12] Stengel, Massimiliano. "Macroscopic polarization from nonlinear gradient couplings." *Physical review letters* 132, no. 14 (2024): 146801. https://doi.org/10.1103/PhysRevLett.132.146801
- [13] Phys. Rev. D. (2023). Multidetector characterization of gravitational-wave burst tensor polarizations. *Physical Review D*, 111(8), 082002. https://doi.org/10.1103/PhysRevD.111.082002

- [14] Satheesh, Abhiroop, Christoph P. Schmidt, Wolfgang A. Wall, and Christoph Meier. "Structure-preserving invariant interpolation schemes for invertible second-order tensors." *International Journal for Numerical Methods in Engineering* 125, no. 2 (2024): e7373. https://doi.org/10.1002/nme.7373
- [15] Sukri, Suzarina Ahmed, Yeak Su Hoe, and Taufiq Khairi Ahmad Khairuddin. "Study of different order of gaussian quadrature using linear element interpolation in first order polarization tensor." *Malaysian Journal of Fundamental and Applied Sciences* 17, no. 4 (2021): 343-353. https://doi.org/10.11113/mjfas.v17n4.2051
- [16] Sukri, Suzarina Ahmed, Yeak Su Hoe, and Taufiq Khairi Ahmad Khairuddin. "First order polarization tensor approximation using multivariate polynomial interpolation method via least square minimization technique." In *Journal of Physics: Conference Series*, vol. 1988, no. 1, p. 012013. IOP Publishing, 2021. http://dx.doi.org/10.1088/1742-6596/1988/1/012013
- [17] Sollberger, D., & Bokelmann, G. (2022). Automated seismic wave-type classification based on eigenanalysis of six-component polarization covariance matrices. Geophysical Journal International, 230(2), 1303–1315. https://doi.org/10.1093/gji/ggad071
- [18] Wagner, David, Nora Weickgenannt, and Enrico Speranza. "Generating tensor polarization from shear stress." *Physical review research* 5, no. 1 (2023): 013187. https://doi.org/10.1103/PhysRevResearch.5.013187
- [19] Yeh, Li-Hao, Ivan E. Ivanov, Talon Chandler, Janie R. Byrum, Bryant B. Chhun, Syuan-Ming Guo, Cameron Foltz et al. "Permittivity tensor imaging: modular label-free imaging of 3D dry mass and 3D orientation at high resolution." *Nature Methods* 21, no. 7 (2024): 1257-1274. https://doi.org/10.1038/s41592-024-02291-w
- [20] Zeng, Li, Tao Zhang, and Hai-Feng Zhang. "A dual-band transmissive polarization conversion metastructure based on the toroidal dipole-assisted EIT effect." *Nanoscale* 17, no. 13 (2025): 7790-7800.. https://doi.org/10.1039/d5nr00006h